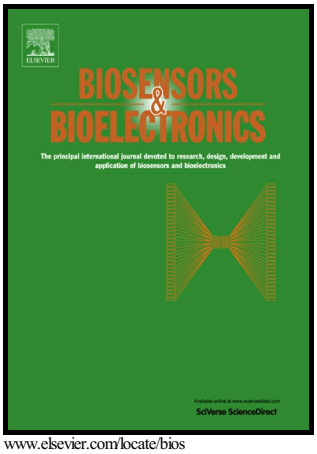

www.elsevier.com/locate/bios

Rapid Detection of Single *E. coli* Bacteria Using a Graphene-based Field-Effect Transistor Device

Bhawana Thakur, Guihua Zhou, Jingbo Chang, Haihui Pu, Bing Jin, Xiaoyu Sui, Xiaochen Yuan, Ching-Hong Yang, Matthew Magruder, Junhong Chen

PII: S0956-5663(18)30178-7
DOI: https://doi.org/10.1016/j.bios.2018.03.014
Reference: BIOS10340

To appear in: *Biosensors and Bioelectronic*

Received date: 1 January 2018
Revised date: 16 February 2018
Accepted date: 6 March 2018

Cite this article as: Bhawana Thakur, Guihua Zhou, Jingbo Chang, Haihui Pu, Bing Jin, Xiaoyu Sui, Xiaochen Yuan, Ching-Hong Yang, Matthew Magruder and Junhong Chen, Rapid Detection of Single *E. coli* Bacteria Using a Graphene-based Field-Effect Transistor Device, *Biosensors and Bioelectronic,* https://doi.org/10.1016/j.bios.2018.03.014

Rapid Detection of Single *E. coli* Bacteria Using a Graphene-based Field-Effect Transistor Device

Bhawana Thakur[a], Guihua Zhou[a], Jingbo Chang[a], Haihui Pu [a], Bing Jin[a], Xiaoyu Sui[a], Xiaochen Yuan[b], Ching-Hong Yang[b], Matthew Magruder[c], and Junhong Chen [a]*

[a]Department of Mechanical Engineering, University of Wisconsin-Milwaukee, 3200 North Cramer Street, Milwaukee, Wisconsin 53211, United States

[b]Department of Biological Sciences, University of Wisconsin-Milwaukee, Wisconsin 53211, United States

[c]Milwaukee Metropolitan Sewerage District, Milwaukee, Wisconsin 53211, United States

ABSTRACT

Contamination of surface and drinking water due to the presence of *Escherichia coli* bacteria is a major cause of water-borne disease outbreak. To address unmet challenges for practical pathogen detection in contaminated samples, we report fabrication of thermally reduced graphene oxide-based field-effect transistor (rGO FET) passivated with an ultrathin layer of Al_2O_3 for real-time detection of *E. coli* bacteria. The sensor could detect a single *E. coli* cell within 50 s in a 1μL sample volume. The ultrathin layer of Al_2O_3 acted as a barrier between rGO and potential interferents present in the sample. *E. coli* specific antibodies anchored on gold nanoparticles acted as probes for selective capture of *E. coli*. The high density of negative charge on the surface of *E. coli* cells strongly modulates the concentration of majority charge carriers in the rGO monolayer, thereby allowing real-time monitoring of *E. coli* concentration in a given sample. With a low detection limit of single cell, the FET sensor had a linear range of 1-100 CFU in 1 μL volume of sample (i.e., 10^3 to 10^5 CFU/ mL). The biosensor with good selectivity and rapid detection was further successfully demonstrated for *E. coli* sensing in river water. The rGO-based FET sensor provides a low cost and label-free

approach, and can be mass produced for detection of a broad spectrum of pathogens in water or other liquid media.

KEYWORDS

Graphene oxide, field-effect transistor, *E. coli*, biosensor, bacteria detection

1. INTRODUCTION

Contamination of drinking and surface water by *Escherichia coli* (*E. coli*) has a profound effect on public health. The acute toxicity associated with Shiga toxins released by the enterohemorrhagic strains of *E. coli* bacteria can cause life-threatening illness amongst the general masses (Edberg et al. 2000; Pandey et al. 2017). Delay in the treatment after the onset of symptoms causes rapid deterioration of patients' health. Hence, real-time monitoring of *E. coli* is essential for disease control and ultimately to safeguard public health. In spite of the fact that gastro intestinal infection is caused by both O157:H7 and non-O157:H7 species of *E. coli*, majority of literature reports focus on detection of O157:H7 strain (Lim et al. 2010). The current methods for detection of *E. coli*, e.g., colony-counting method, consist of multiple steps, require trained personnel and give confirmatory results only after 24-48 h (Bulard et al. 2015). Recent amplification-based molecular diagnosis methods like polymerase chain reaction (PCR) can reduce the assay time to hours. However, even the combination of PCR and colony-counting methods is not sensitive enough to detect bacteria at low concentrations ($\ll$1–100 colony-forming units per mL (CFU/ mL) of sample) (Kang et al. 2014; Lee et al. 2007). Moreover, to achieve a low detection limit, PCR requires an additional enrichment step. For practical applications, the detection platform should be ultrasensitive because even a single cell of bacteria can cause serious illness. The conventional methods also suffer from poor specificity and high background signals due to the turbidity and presence of non-target species in real samples. Therefore, the existing

methods for *E. coli* detection not only require expensive equipment and special training but are also time consuming and less sensitive. To address these limitations, it is important to develop a sensitive, rapid, and cost-effective sensor platform to detect *E. coli* in drinking and surface water.

There are several literature reports based on the combination of various techniques and smart materials for the detection of *E. coli* contamination in both food and water. Majority of these detection techniques are based on optical, electronic and electrochemical methods which offer rapid response and ease of operation (Acharya et al. 2006; Chen et al. 2017; Labib et al. 2012; Pandey et al. 2017). However, optical methods often use chromogenic or fluorescent probes and the turbidity of sample matrix affects both sensitivity and detection limit (Miranda et al. 2011; Wang et al. 2012; Yoo and Lee). In the case of electrochemical detection methods, requirement of electro-active substrates or electro-active labels in addition to the background signal associated with various interfering species limit the application for *E. coli* detection in real samples (Zhu et al. 2015). In addition, *E. coli* detection is also reported based on various methods like real-time mass spectrometry and piezoelectric techniques (Campbell and Mutharasan 2007; Li et al. 2010). Over the years, field-effect transistors (FETs) have become a very attractive choice for sensing applications due to their rapid response, high sensitivity, good reproducibility and real-time monitoring compared with several other detection techniques (Chang et al. 2013a; Chang et al. 2013b; Chang et al. 2015; He et al. 2012; Zang et al. 2016; Zhou et al. 2014; Zhu et al. 2015). Usually materials like carbon nanotubes, graphene, and silicon nanowires are integrated as active channel along with suitable probe molecules into an FET device for sensing applications (Ahn et al. 2010; Allen et al. 2007; Liu and Guo 2012). Amongst various channel materials, graphene holds great promise as transducer in FET-based sensors. Graphene is a low electronic noise 2D system with low contact resistance, wherein the whole volume is available for interactions

with the analyte (Geim and Novoselov 2007; Schedin et al. 2007; Zhang et al. 2005). Along with desirable properties like high electron mobility, excellent thermal conductivity, and large surface-to-volume ratio, graphene exhibits high capacitance, and tunable ambipolar field-effect characteristics (Zhou et al. 2014). This has prompted the application of graphene-based FET for sensing of plethora of analytes like heavy metal ions, pathogens, proteins, and nucleic acids (Cai et al. 2014; Chang et al. 2013b; Chang et al. 2015; Martínez et al. 2009; Ohno et al. 2010; Zhou et al. 2014).

Herein we have developed a thermally-reduced graphene oxide (rGO)-based FET platform modified with *E. coli* antibodies (anti- *E. coli)* for detection of single *E. coli* bacteria. To detect more than one strain of *E. coli*, generic anti- *E. coli* were used as a probe. The active channel is thermally-reduced graphene oxide (GO) sheet which is deposited on Au/ SiO_2 based electrode surface via chemical modification. Presence of oxygen-containing functional groups like epoxy, hydroxyl, and carboxyl enables chemical modification of substrates with GO. GO is a less expensive derivative of graphene that can be easily reduced either by a chemical method or thermal annealing. The sensing mechanism of graphene-based FETs relies on change in the electrical conductivity of the rGO channel upon binding with the *E. coli* because *E. coli* has net negative charge around its membrane, which modulates the conductivity of rGO in FET. To passivate the rGO channel, the FET is modified with few nanometre thick Al_2O_3 layer using an Atomic Layer Deposition (ALD) technique. The Al_2O_3 layer inhibits any direct contact of water or unwanted species with the rGO surface without affecting its FET characteristics, which improves the reproducibility and stability of the sensor. This sensor platform is capable of detecting a single *E. coli* cell. The sensor could also detect *E. coli* in river water sample, which proves its potential for practical applications in point-of-use sensing.

2. EXPERIMENTAL METHODS

2.1. Materials

$KMnO_4$, $NaNO_3$, H_2SO_4, glutathione (GSH), α-ethyl-tryptamine (AET), 1-Ethyl-3-(3-dimethylaminopropyl)-carbodiimide (EDC), N-Hydroxysuccinimide (NHS),and the blocking buffer (0.1% Tween 20) were purchased from Sigma-Aldrich. Purified natural graphite was purchased from SP-1 BayCarbon, MI. Thiol Green Indicator Assay kit was procured from abcam. Micro-BCA Protein Assay Kit was purchased from ThermoFisher Scientific. Heat killed *Salmonella typhimurium* and *Streptococcus pneumonia* were procured from InvivoGen. *E. coli* serotype O/K polyclonal antibody (anti-*E. coli*) was purchased from ThermoFisher Scientific. The *E. coli* (ATCC 25922) strains were grown in LB medium (1% tryptone, 0.5% yeast extract, and 1% NaCl) at 37°C for 12h.The concentration of saturated culture was estimated by a plate counting method and UV- vis spectrophotometer. Prior to sensing, the culture was washed with DI water and centrifuged to remove growth medium. The culture was resuspended in DI water and diluted to obtain desired concentrations. River water samples supplied by Milwaukee Metropolitan Sewerage District (MMSD) were used without any pre-treatment.

2.2. GO Synthesis

The modified Hummer's method was used for the synthesis of GO (Marcano et al. 2010). The purified natural graphite was subjected to oxidization in the presence of $KMnO_4$ and $NaNO_3$ in concentrated H_2SO_4. The GO dispersion was centrifuged to remove possible agglomeration materials followed by subsequent washing in DI water. The stable suspension of GO sheets of required concentration was obtained after ultasonication.

2.3. Device Fabrication

The step wise fabrication is shown in schematic (**Figure 1**). The Au interdigitated electrodes with 2 mm length and 50 nm thickness were fabricated using a photolithographic process on

a highly doped Si wafer with an upper layer of dry-formed SiO_2(thickness of 200 nm).The finger-width and inter-finger spacing of electrodes was 2 µm. The self-assembly of thiol was used to anchor GO on the interdigitated Au electrodes. The electrode was modified with AET (1 mg/mL for 10 min) to give amine-terminated functionality. The amine-terminated electrodes were immersed in the GO solution for 10 minutes followed by washing with copious amount of deionised water. The electrodes with self-assembly of GO were then subjected to thermal annealing in a tube furnace (Lindberg Blue, TF55035A-1) by heating the device for 10 min at 400 °C in Ar flow of 1 litre/min. A thin layer of Al_2O_3 (3 nm) was coated over the rGO-modified electrodes using ALD. To anchor the anti- *E. coli*, Au nanoparticles (NPs) were sputter coated on the FET for 3 s using an RF (60 Hz) Emitech K550x sputter coater apparatus with an Au target (99.999% purity), at an Ar pressure of 0.03 mbar and a working current of 20 mA. 5 µL of GSH solution (10 mM) was dropcasted on electrodes for 1 h. The carboxylic acid functionalized electrodes were then linked with anti-*E. coli* with the help of EDC- NHS chemistry. For this purpose, 5 µL of 1:1 mixture of EDC and NHS solution (20 mM) was dropcasted on electrodes for 30 min. The electrode with the reactive ester group was kept for overnight modification with anti-*E. coli* at 4 $^{\circ}$C. The total loading of anti- *E. coli* on the sensor was determined using bicinchoninic acid (BCA) protein assay (**Figure S1**). Such type of analysis is important to obtain batch-wise quality control for reproducibility. To avoid non- specific binding, the sensors were finally incubated in a blocking buffer for 1 h at room temperature followed by washing with the DI water. The fabricated sensors were stored at 4 $^{\circ}$C in dry airtight containers.

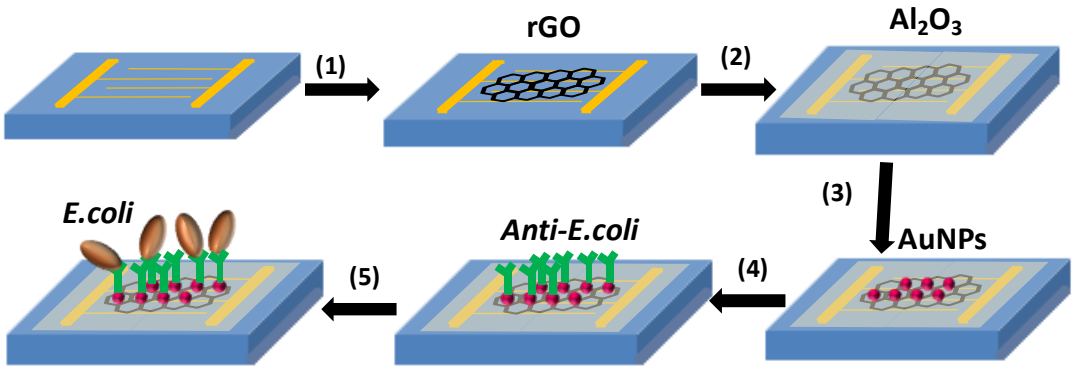

(1) Self assembly of rGO followed by thermal reduction , (2) Deposition of atomic layer of Al_2O_3, (3) Deposition of AuNPs, (4) Immobilization of Anti-*E. coli*, and (5) *E. coli* sensing

Figure 1: Schematic depicting various steps involved in the fabrication of anti- *E.coli*/ AuNPs/ Al_2O_3/ rGO FET sensor.

2.4. Measurement and Characterization:

Atomic force microscopy (AFM) was recorded by Agilent Technology 5420 AFM with a cantilever (Nanosensors PPP-NCH). Electrical and transport measurements were performed on the sensors using a Keithley 4200 semiconductor characterization system. X-ray photoelectron spectroscopy (XPS) spectra of GO samples were obtained using an HP5950A ESCA spectrometer with monochromatic Al Kα radiation as X-ray source. With a back-gate applied to the FET device at room temperature, the source- drain current (I_{SD}) was measured as a function of the gate voltage (V_{gs}) and the source-drain voltage (V_{ds}). The gate bias was varied from −40 to +40 V. The electrical conductivity of the sensor was recorded by monitoring the change in the drain current (I_{SD}) with a fixed V_{ds} for various concentrations of *E. coli* solutions. Hitachi S4800 field-emission scanning electron microscope (SEM) at a 2 kV acceleration voltage was used to characterize the sensors after every fabrication step. The Infinite 200 PRO (Tecan) plate reader was used for the bicinchoninic acid (BCA) assay and to determine amount of GSH on sensors.

3. RESULTS and DISCUSSIONS

3.1. Sensor Characterization

Due to the facile method of fabrication we could easily control the quality of rGO on our sensors. Prior to the immobilization of GO on Au electrodes, GO dispersion was subjected to sonication to obtain monolayers. The weak binding between layers of GO allows easy separation of GO into monolayers during sonication. Sonication time and power was optimized to obtain monolayer dispersion with uniform size of GO sheets. GO was self assembled on Au interdigited electrode with AET as linker molecule. The strong affinity of thiol group in AET towards Au aids formation of self assembled monolayers (SAM) of AET on interdigited electrode. The amine end of AET the binds with various functional groups present in GO monolayers (carboxylic acid, and epoxide) via electrostatic adsorption. Assembly time of GO solution on AET modified Au electrodes was optimized to control the coverage area of sensor. Followed by self assembly of GO, the devices were subjected to thermal annealing under argon atmosphere (400 °C with argon flow of 1 litre/min). Thermal reduction under argon atmosphere improves the semiconducting property of GO by reducing the oxygen-containing groups in GO monolayer. Moreover, this process also decreases the junction barriers between the Au electrodes and rGO. Followed by the thermal reduction, to passivate rGO, Al_2O_3 layer (3nm) is deposited over the FET with the help of ALD technique. To immobilize *anti- E. coli* (probe molecule) on the FET, we used AuNPs as the anchoring sites. Owing to the chemical inertness, and facile methods of functionalization, AuNPs are ideal candidates for immobilization of bio-recognition elements during fabrication of biosensors. Functionalised AuNPs conjugated with antibodies have been reported for sensing and imaging (Jazayeri et al. 2016). In our work, we have functionalised AuNPs with GSH followed by EDC/ NHS binding. The thiol group on GSH binds to AuNPs through electrostatic interaction and the terminal carboxylic acid group at the other end of GSH

molecule is converted to reactive ester by EDC/ NHS reaction. The reactive ester group then combines with amine groups on *anti- E. coli*, thereby immobilizing it on FET sensors.

The thickness of deposited GO sheet on electrode (~1.2 nm) was measured using AFM (**Figure S2**). Since the thickness of a single-layer graphene oxide sheet is~ 1.1 nm, the AFM measurement suggests that the GO sheet on our sensor is monolayer (Zhou et al. 2014). **Figure S2** shows FTIR spectra of GO at 25 ^{o}C and post thermal annealing at 400^{o}C. GO contains various oxygen functionalities which appear in the FTIR spectra (3400 cm^{-1} for O-H stretching vibrations, 1720 cm^{-1} for C=O stretching vibrations, 1600 $cm^{-1}$for C=C stretching vibrations, 1220 cm^{-1} for C-OH stretching vibrations, and 1060 cm^{-1} for C-O stretching vibrations) (Choi et al. 2010; Kellici et al. 2014). The spectra of GO after thermal annealing showed significant decrease in the absorption peak of C=O (1720 cm^{-1}), while band for C–OH stretching vibrations at 1220cm^{-1} disappeared completely. This decrease in oxygen containing functionalities confirmed reduction of GO due to thermal annealing at 400^{o}C under argon atmosphere. The XPS spectra of GO and rGO, which shows increase in C/O ratio after thermal annealing also confirmed the reduction of GO (**Figure S3**).

The SEM image of monolayer rGO sheets bridging the gap between the Au interdigitated electrodes is shown in **Figure 2a**. The inset of **Figure 2a** shows the uniform distribution of Au NPs on the surface of the rGO sheet protected with a 3 nm thick layer of Al_2O_3. The electrical properties of rGO FETs were measured at room temperature using the back-gated FET devices (**Figure 2b**). For this purpose, the source-drain current (I_{SD}) was measured while the gate bias (V_{gs}) was varied from -40 to +40 V. The p-type semiconducting property of rGO FET is evident from the decrease in conductivity with increasing voltage.

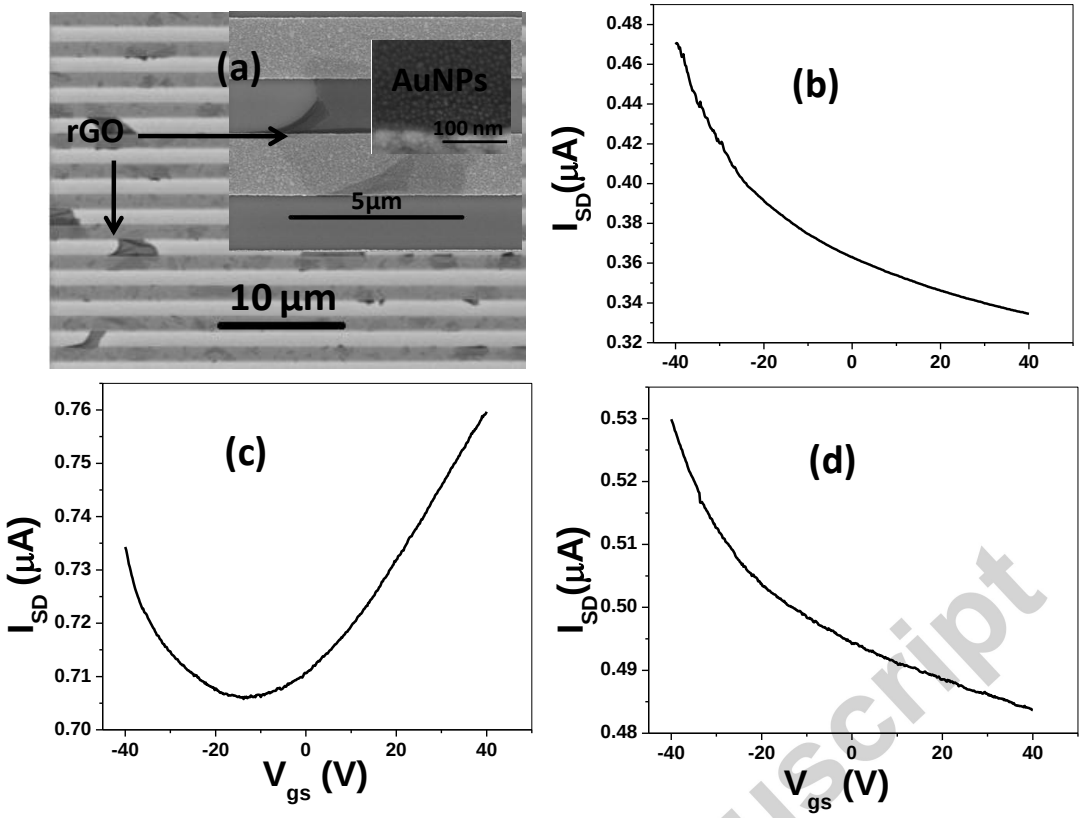

Figure 2:(a) SEM images of AuNPs/ Al_2O_3/ rGO FET**, (b)** I_{SD}−V_{gs} characteristics of rGO FET, **(c)** Al_2O_3/ rGO FET**,** and **(d)** anti- *E. coli*/ AuNPs/ Al_2O_3/ rGO FET (V_{ds} = 0.01 V, V_{gs} = −40 to 40 V, step = 0.2 V).

The abundance of defects in the rGO has also been demonstrated with the help of Raman spectrum in the previous reports, which showed that the D band is higher than the G band in rGO (Ghosh et al. 2012; Zhou et al. 2014). Further, the Al_2O_3-protected rGO FET showed bipolar FET characteristics (**Figure 2c**). This can be attributed to the presence of electrons (introduced by Al_2O_3), which now in addition to holes act as charge carriers. A similar type of phenomenon was reported by Schmid et al (Schmid et al. 2006). Ultrathin layers of Al_2O_3 possess oxygen (O) vacancies. Due to these vacancies, two Al 3*p* electrons fail to find the corresponding empty O 2*p* conduction band states. In the present case, the rGO layer beneath it acts as potential electron reservoir. Thus in addition to holes, rGO sheets have added electrons which contribute to the FET characteristic of the sensor. The FET characteristic of

the sensor reverts back to p- type after modification with antibodies. This could be because of positively charged antibodies which pull the electrons from Al_2O_3 layer, thereby reducing their concentration in the rGO sheet (**Figure 2d**).

We also investigated the effect of size and number of AuNPs on adsorption of linker molecule on the surface of FET sensor. AuNPs provide binding site for anti- *E. coli* via linker molecule i.e., GSH in our study. Thus it is important to immobilize maximum amount of GSH on the FET sensor. Additional studies were carried out to improve the adsorption capacity of the AuNPs and the areal density of GSH. A group of control experiments were conducted for six AuNPs samples with different sputtering parameters (**Table S1**). The morphology of AuNPs in each sample was characterized with SEM to measure the size and number of particle on the sensing surface. Increasing the sputtering time increases the number of AuNPs and higher sputtering current gives larger particle size. Since the sputtering current of 25 mA resulted in congregation of particles (sample No.6), we did not extend our study above this current range. The areal density ($=N\times\pi D^2$) was defined as the indicator for effective adsorption surface. Each group of sample has 1.5 cm×1.5 cm silicon wafers (*n=4* for each group), which was submersed in 1 mL of GSH solution (50 μM). After 1 h, the silicon wafers were taken out, and the remaining concentration of GSH in the solution was measured with fluorescence plate reader by using Thiol Green Indicator test (**SI**). **Figure S4** shows the correlation between GSH adsorption and AuNPs size, count and areal density. From this study it can be concluded that compared to particle size or particle number, adsorption of GSH has higher dependency on areal density of AuNPs. Therefore, balancing the size and number of AuNPs to achieve a uniform sensing surface with a maximum areal density is the key to maximize the probe adsorption. For this purpose, both current and sputter coating time were optimized to get the desired areal density of AuNPs on the surface of sensor. Further, the concentration of linkers (GSH, EDC/ NHS) was also optimized to

immobilize maximum amount of *anti- E. coli* on the surface of sensor. The amount of *anti- E. coli* was estimated by BCA protein assay (**SI**). The concentration of GSH was varied from 2 mM to 15 mM with corresponding two fold higher concentrations of EDC/ NHS. The amount of immobilized *anti- E. coli* increased sharply for 2 mM to 10 mM of GSH. Increase in concentration of GSH beyond 10 mM did not have any further effect on the concentration of immobilized *anti- E. coli* (**Table S2**).

3.2. Sensing Performance

The *E. coli* FET sensor is fabricated on Au electrodes with rGO as the conducting channel. In the FET, rGO is bridging the source and drain electrodes. Under normal conditions GO is electrically insulating due to the presence of saturated sp3 bonds, the high density of electronegative oxygen atoms bonded to carbon, and other defects give that rise to an energy gap in the electron density of states. After thermal reduction, due to larger sp^2 domains rGO becomes electrically conducting and the FET sensor shows resistance between 50 kΩ to 150 kΩ (Jung et al. 2008; Kumar et al. 2016). The sensing of *E .coli* is dependent on modulation of electrical conductivity of rGO in FET sensor. In the absence of rGO or prior to reduction of GO, the FET behaves like an open circuit and does not respond to addition of the analyte. We also studied the effect different thickness of Al_2O_3 layer (1nm, 2nm, 3nm, 4nm) on the performance of FET sensor. For Al_2O_3 layer below 3nm, the sensors were quite unstable and susceptible to oxidation. Owing to the Debye length limitation, for thickness above 3nm the devices became inert to external environment and do not respond to the addition of analyte (Wu et al. 2016).

For sensing experiments, the sensor was subjected to various concentrations of *E. coli* in DI water (10^3 CFU/ mL to 10^9 CFU/ mL).1 µL of sample volume was used for analysis. The actual number of *E. coli* detected on the sensor depends on both the concentration of *E. coli* and the sample volume used for analysis. Calculation to estimate the number of *E. coli* cells

dropcasted on the sensor surface for various concentrations of sample solutions is shown in **Table S3**. Although the lowest concentration of *E. coli* sample used for sensing is 10^3 CFU/ mL, based on the calculations the sensor is detecting a single *E. coli* cell.

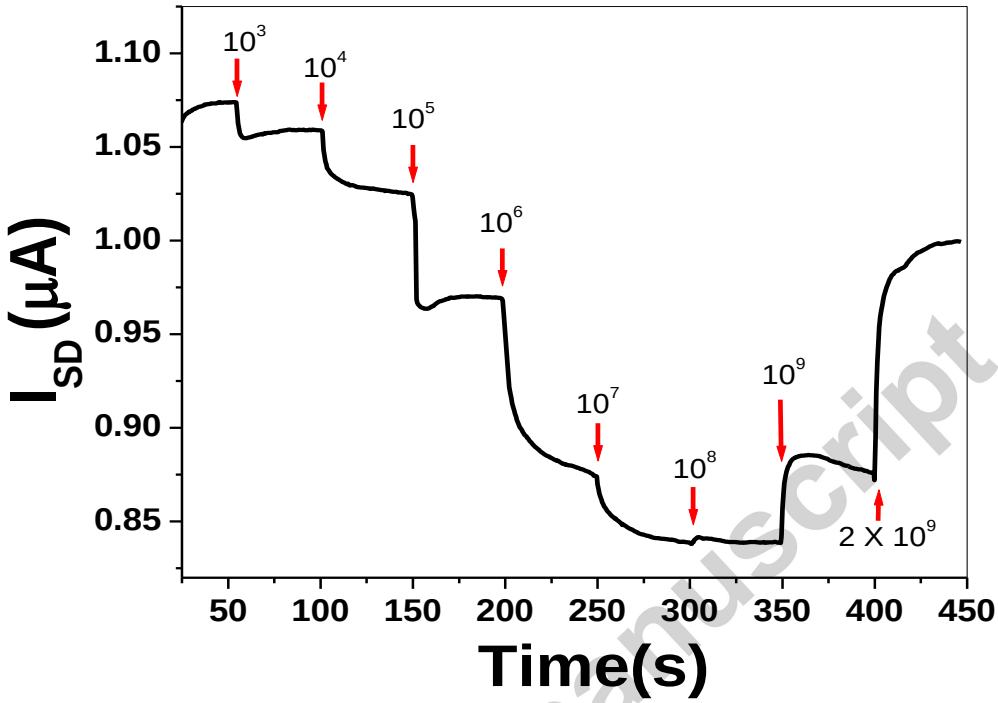

Figure 3: Real-time detection (V_{ds} = 0.1 V) of *E.coli* (CFU/ mL) in water with the anti- *E. coli*/ AuNPs/ Al_2O_3/ rGObiosensor.

The anti- *E. coli* anchored on the surface of AuNPs selectively captures *E. coli* cells. The capture of *E. coli* cells by anti- *E. coli* from the sample is reflected by the change in the electrical conductivity of the rGO channel, i.e., I_{SD}. **Figure 3** shows the real-time monitoring of *E. coli* by the sensor. There is a linear decrease in I_{SD} after the addition of *E. coli* aliquot from 10^3 CFU/ mL to 10^6 CFU/ mL. Alternatively, the I_{SD} increases after addition of 10^7 CFU/ mL of *E. coli* solution. The sensor has a rapid response time for the *E. coli* detection. A short response time is one of the important advantages of FET sensors. One of the previous works reported by our group based on rGO FET for detection of Pb^{2+} ions also had a very quick response. This was attributed to the rapid diffusion of ions from the liquid drop on the

surface of the device to the contact area (Zhou et al. 2014). Although *E. coli* is very much larger than ions or molecules, the low volume of sample reduces the diffusion length and enables rapid analysis of samples. The reported methods for *E. coli* detection usually involved minimum 30 minutes of incubation time after multiple sensor fabrication steps (Hassan et al. 2015; Laczka et al. 2008). Moreover, such methods of analysis are unsuitable for real-time analysis of samples like flowing water or other samples where continuous monitoring of water purity is essential. We also carried out control experiments with the sensor which did not have any probes, i.e., anti- *E. coli*. The sensor for control experiments was AuNPs/ Al_2O_3/ rGO FET. Addition of *E. coli* did not generate any signal, which proves that the anti- *E. coli* FET sensor responds only after specific binding with *E. coli* (**Figure S5**). The sensing mechanism in the present case can be attributed to the synergistic effect between the Al_2O_3 layer and the rGO channel, the conductivity of which is modulated upon coming in contact with negatively-charged *E. coli* cells. The rGO layer is the potential electron reservoir for the free electrons since the oxygen vacancies in Al_2O_3 fail to find the corresponding empty O 2*p* conduction band states. In other words, the oxygen vacancies lead to the dangling bonds in aluminium atoms, which can act as electron donors. The 1-2 µm sized *E. coli*, which has rich density of negative charge on its surface, is in close vicinity with the surface of electron-rich Al_2O_3 layer. This cloud of negative charge further enhances the electron donating capability of Al_2O_3. To restore its insulating property, the oxygen-deficient domain boundary of Al_2O_3 behaves like a native electron donor and rGO sheets acts as recipient (Schmid et al. 2006). The majority carriers (i.e., holes) in the rGO sheet combine with these electrons. This reduction in the concentration of majority charge carriers decreases the current flow between source and drain. In addition, the sensing mechanism can be associated with the gating effect of the *E. coli* antibodies present on the sensor surface. The antibodies lose positive charge which is induced by adsorption of negatively-charged *E. coli*

cells. The magnitude of the positive charge on antibodies decreases with the increasing concentration of *E. coli*. This decreased positive charge of the antibodies indicates that the AuNPs are less negatively charged since the antibody itself can work as a dielectric medium. As a result, the concentration of holes in the rGO sheet from the gate-insulator/semiconductor interface, i.e., the current flow between source and drain decreases upon adsorption of *E. coli*. Above a threshold concentration of 10^7 CFU/ mL, there are excess of *E. coli* cells in the sample solution. Rather than coming in direct contact with the Al_2O_3 layer, *E. coli* cells stack over each other. An additional experiment has been carried out to monitor the effect of *E. coli* concentration on conductivity of DI water **(Table S4)**. It was observed that the conductivity of DI water increases exponentially with increasing concentration of *E. coli*. The effect of concentration on the conductivity of DI water is more pronounced after 10^6 CFU/ mL concentration of *E. coli*. The observed trend is due to the accumulation of *E coli* cells in the sample solution, which increases the ionic conductivity of the DI water leading to increase in I_{SD}. This increase in conductivity can be attributed to the surface charge present on the membrane of *E. coli* cells. The high density of these negatively charged groups directly affects the rGO in FET by acting as gate electrolyte that exerts negative potential. This in turn generates more holes in the rGO channel thereby increasing the I_{SD} of FET sensor. Thus there are two competing effects wherein one leads to decrease in current (10^3 CFU/ mL to 10^6 CFU/ mL) and other causes increase in current (10^6 CFU/ mL to 10^9 CFU/ mL). By looking at the graphs for real time detection of *E. coli* (**Figure 3 and 4**) and the values for conductivity (**Table S4**), it can be inferred that effect of solution conductivity on FET signal due to increasing concentration of *E. coli* is more pronounced after addition of 10^6 CFU/ mL of cells. Although, **Figure 3** shows significant decrease in I_{SD} after addition of 10^6 CFU/ mL, instead of 10^3 CFU/ mL to 10^6 CFU/ mL the graph has good linear fitting from 10^3 CFU/ mL to 10^5 CFU/ mL. Thus, effect of conductivity below 10^5 CFU/ mL on FET sensor, even if any

can be neglected. The calibration plot showing linear relation between % response (%R) and concentration of *E. coli* is shown in **Figure 4.** The response is linear from 10^3 CFU/ mL to 10^5 CFU/ mL of *E. coli* concentration. This work has focused on a concentration range of *E. coli* below 10^6 CFU/ mL. Besides, there are some commercial kits which can detect presence of bacteria, especially of coliforms with 10^5 CFU/ mL as lowest possible detection limit. It is more challenging to detect concentration of bacteria below 10^5 CFU/mL, which is important for practical applications.

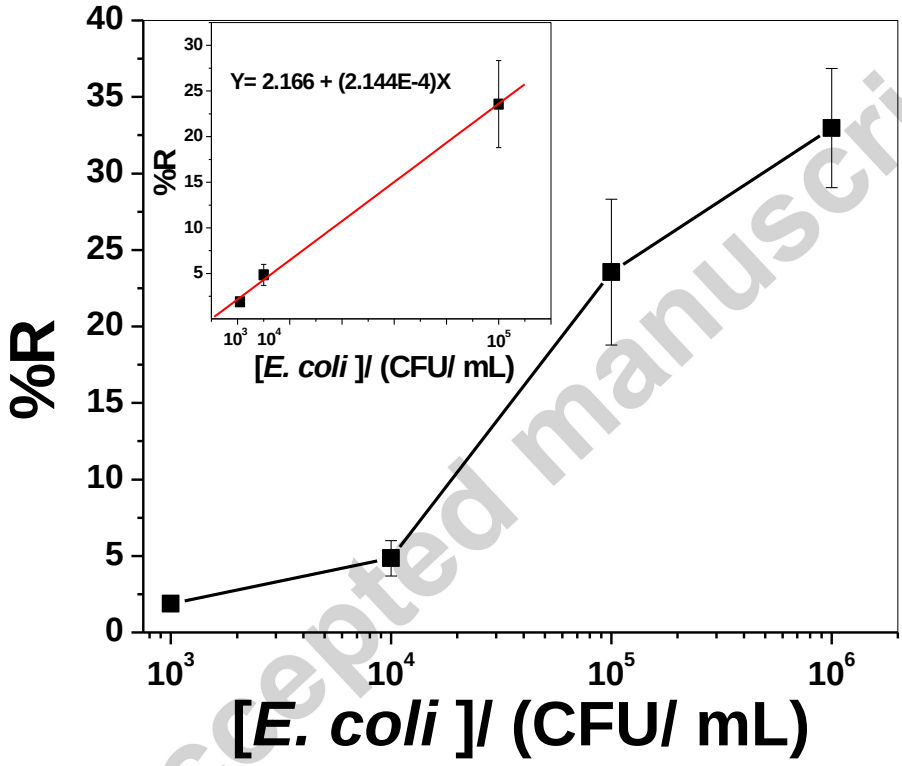

Figure 4: The response curve of anti- *E. coli*/ AuNPs/ Al_2O_3/ rGO biosensor to *E. coli* addition, where % R= [(Resistance$_{final}$-Resistance$_{initial}$)/Resistance$_{initial}$]*100. Inset: Linear fitting from 10^3 CFU/ mL to 10^6 CFU/ mL of *E. coli* concentration.

The distribution of *E. coli* cells on the surface of sensors at various concentrations is shown in **Figure 5.** The detailed calculation showing number of *E. coli* dropcasted on the sensor is

shown in **Table S3**. The SEM image of *E. coli* cells on sensor surface is recorded over a very small portion of electrode surface. The total area of electrode is 0.24 mm (0.8mm × 0.3 mm) on which *E. coli* cells are distributed. To make *E. coli* visible in the image we have focused on very small area of the electrode and hence the visible number of cells in the images is far less than the total number of cells dropcasted on sensor. As seen from the SEM images, from 10^6 CFU/mL onwards the sensor has a dense coverage of *E. coli* which causes saturation in the sensor response. Although the lowest concentration of *E. coli* to which the sensor is responding is 10^3 CFU/mL, 1 µL of the sample droplet has a single CFU of *E. coli* or a single *E. coli* cell. It may be noted that since the sample volume used for analysis in our work is 1µL, the sensor is thus capable of detecting a single *E. coli* cell. Coupling of this platform with a filtration setup can easily help in detection of single or few *E. coli* cells in a larger volume of samples. It is strictly required in drinking water that *E. coli* must not be detectable in any 100 mL sample. Thus, for such type of practical applications it is very important for a sensing platform to detect as low as a single bacterial cell. The rGO-based FET sensor reported in this work has shown a tremendous potential for this application as it can precisely detect a single *E. coli* cell in a given sample. There are very few literature reports where the sensor was able to detect as low as a single cell (Hahn et al. 2005; Kang et al. 2014; Sepunaru et al. 2015; Zhao et al. 2004). The performance of these sensors with respect to the linear range, detection time, and detection limit are summarised in **Table S5** in supporting information.

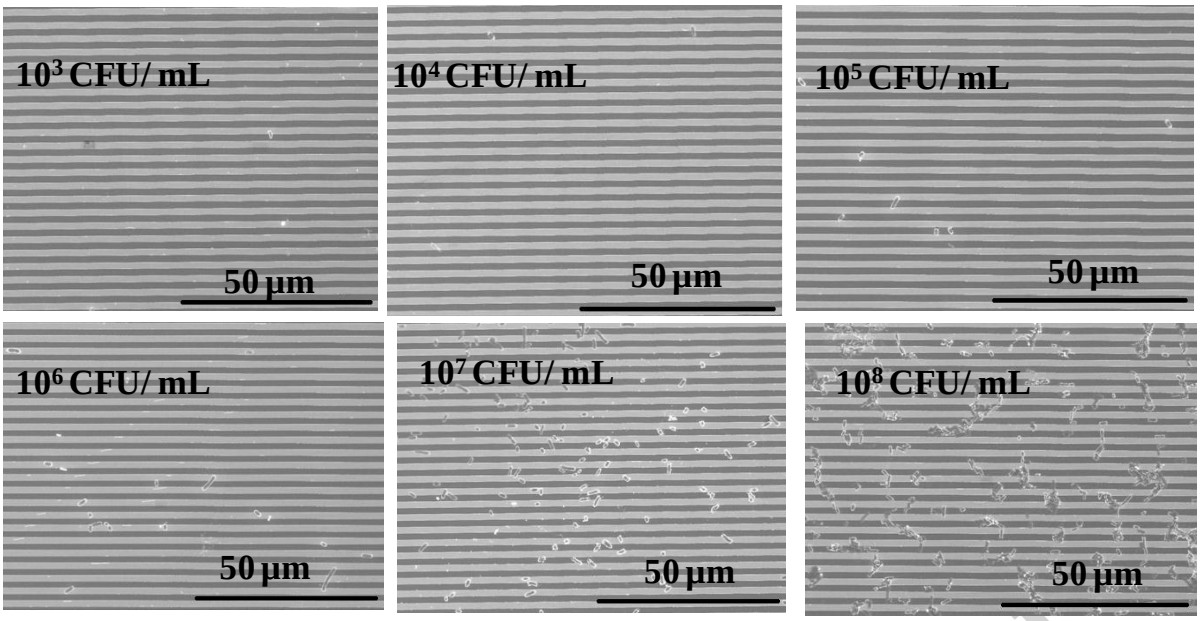

Figure 5: SEM images showing distribution of *E. coli* dropcasted on the anti- *E. coli*/ AuNPs/ Al_2O_3/ rGO biosensor.

Further, the electrostatic self-assembly of GO on amino-terminated Au electrode allowed precise control of uniformity of the GO film which in turn contributed to the stability of device. When preserved at a storage temperature of 4 °C, the *E. coli* FET sensors did not show any significant deterioration in performance after 14 days of fabrication. These sensors are designed for one time use. As far as stability of sensor with respect to reusability is concerned, the very small sensing area of FET sensor is not suitable for regeneration. However, suitable reagents (for e.g. buffers) can aid the complete regeneration of sensor surface without affecting the FET performance. The stability of the *E. coli* FET sensors in terms of reusability needs further investigation. The sensing experiments were carried out at 25 °C. Increase in temperature will positively affect the conductivity of rGO. Since our sensor is targeted for room temperature analysis we did not extend our studies for range of temperature.

3.3. Interference Test and Real Sample Analysis

The sensor uses anti- *E. coli* which makes its highly specific to target i.e., *E. coli*. River water can have various species of bacteria. Instead of testing whole array of these species we have performed interference test with two commonly occurring bacteria- *Salmonella typhimurium* and *Streptococcus pneumonia*, each from gram negative and gram positive species of bacteria. The commercially available antibodies like *anti- E. coli* are raised against surface protein of bacteria. These surface proteins which have site- specific binding sites for antibodies are present on the outer membrane of bacteria, and are retained even in heat killed-bacteria (Vanaja et al. 2016). Hence, although we have used dead bacteria for interference tests, similar results can be expected with live cells. To evaluate the reliability of the sensing platform, interference tests were performed by monitoring the response of *E. coli* in the presence of heat killed *Salmonella typhimurium* and *Streptococcus pneumonia*. For this purpose, the dynamic response of the sensor to a mixture of *E. coli* (10^4 CFU/ mL) +heat killed *Salmonella typhimurium* (10^6 cells/ mL) and *E. coli* (10^4 CFU/ mL) + heat killed *Streptococcus pneumonia* (10^6 cells/ mL) was monitored. The presence of the bacteria apart from *E. coli* did not influence the signal. This proves that the sensor is specific to *E. coli* which can be attributed to the *E. coli* antibodies that selectively capture *E. coli* cells from the sample to generate the response (**Figure 6**).

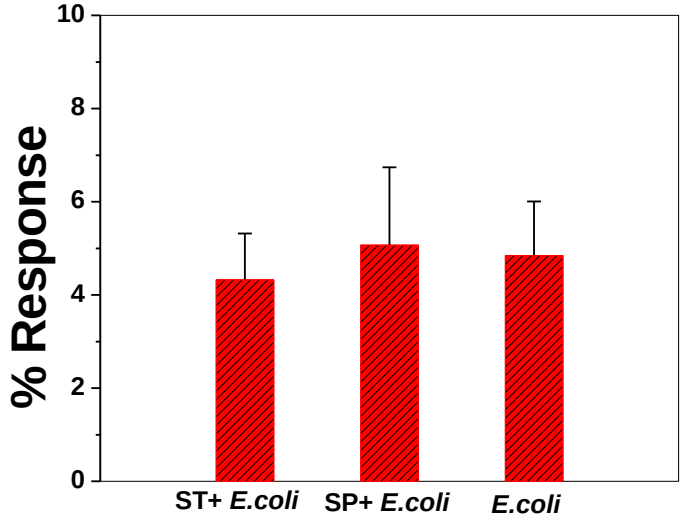

Figure 6: Bar chart depicting selectivity of anti- *E. coli*/ AuNPs/ Al_2O_3/ rGO biosensor for *E. coli* in the mixture of *E. coli* (10^4 CFU/ mL) + heat killed *Salmonella typhimurium* (10^6 cells/ mL) and *E. coli* (10^4 CFU/ mL) + heat killed *Streptococcus pneumonia* (10^6 cells/ mL). Presence of the bacteria apart from *E. coli* did not have any significant impact on the % response. *ST: *Salmonella typhimurium*, SP: *Streptococcus pneumonia*

The proposed analytical protocol was also applied to determine the *E. coli* concentration in river water samples spiked with increasing concentrations of *E. coli*. Since river water has lot of potential interfering species (like metal ions, organic matter, etc.), contrary to deionised water wherein the detection limit was 10^3 CFU/ mL the sensor was able to detect 10^4 CFU/ mL of *E. coli* in real time in river water **(Figure S6)**.

4. CONCLUSION

This study has reported the fabrication and application of anti - *E. coli*/AuNPs/Al_2O_3/rGO/ FET sensor for the detection of *E. coli*. The sensing relies on modulation in the conductivity of rGO channel of the FET after coming in contact with *E. coli*. The sensor had a rapid response and is very selective to *E. coli* with potential of detecting single *E. coli* cell in a large volume of sample when coupled with a suitable filtration setup. These sensors are

designed for one time use and the results indicate very good stability of the sensor during the entire course of measurement of electrical conductivity. The sensor showed good reproducibility for *n=3* measurements. Moreover, the sensor could detect *E. coli* in a complex matrix of river water sample, promising its practical applications. The sensor is designed for one-time use and has the possibility of regeneration by using a suitable regeneration buffer. These disposable, low cost, and robust sensors can be readily mass produced. This approach can be utilized for detection of other bacteria by incorporating appropriate probe molecules, i.e., antibodies during the sensor fabrication. The performance of this new genre of bacteria sensors is either superior or comparable to most of the highly sensitive bacteria sensors reported in literature. We are further exploring the potential of the sensor for its ability to differentiate between dead and viable *E. coli* cells.

Acknowledgements

This work was supported by the U.S. National Science Foundation (NSF) through an NSF Industry/University Cooperative Research Centre Grand Challenge Grant and MMSD. River water samples and lab results were provided by MMSD.

REFERENCES

Acharya, G., Chang, C.-L., Savran, C., 2006. An Optical Biosensor for Rapid and Label-Free Detection of Cells. Journal of the American Chemical Society 128(12), 3862-3863.

Ahn, J.-H., Choi, S.-J., Han, J.-W., Park, T.J., Lee, S.Y., Choi, Y.-K., 2010. Double-Gate Nanowire Field Effect Transistor for a Biosensor. Nano Letters 10(8), 2934-2938.

Allen, B.L., Kichambare, P.D., Star, A., 2007. Carbon Nanotube Field-Effect-Transistor-Based Biosensors. Advanced Materials 19(11), 1439-1451.

Bulard, E., Bouchet-Spinelli, A., Chaud, P., Roget, A., Calemczuk, R., Fort, S., Livache, T., 2015. Carbohydrates as New Probes for the Identification of Closely Related Escherichia coli Strains Using Surface Plasmon Resonance Imaging. Analytical Chemistry 87(3), 1804-1811.

Cai, B., Wang, S., Huang, L., Ning, Y., Zhang, Z., Zhang, G.-J., 2014. Ultrasensitive Label-Free Detection of PNA–DNA Hybridization by Reduced Graphene Oxide Field-Effect Transistor Biosensor. ACS Nano 8(3), 2632-2638.

Campbell, G.A., Mutharasan, R., 2007. A Method of Measuring Escherichia Coli O157:H7 at 1 Cell/mL in 1 Liter Sample Using Antibody Functionalized Piezoelectric-Excited Millimeter-Sized Cantilever Sensor. Environmental Science & Technology 41(5), 1668-1674.

Chang, J., Mao, S., Zhang, Y., Cui, S., Steeber, D.A., Chen, J., 2013a. Single-walled carbon nanotube field-effect transistors with graphene oxide passivation for fast, sensitive, and selective proteindetection. Biosensors and Bioelectronics 42, 186-192.

Chang, J., Mao, S., Zhang, Y., Cui, S., Zhou, G., Wu, X., Yang, C.-H., Chen, J., 2013b. Ultrasonic-assisted self-assembly of monolayer graphene oxide for rapid detection of Escherichia coli bacteria. Nanoscale 5(9), 3620-3626.

Chang, J., Zhou, G., Gao, X., Mao, S., Cui, S., Ocola, L.E., Yuan, C., Chen, J., 2015. Real-time detection of mercury ions in water using a reduced graphene oxide/DNA field-effect transistor with assistance of a passivation layer. Sensing and Bio-Sensing Research 5, 97-104.

Chen, J., Andler, S.M., Goddard, J.M., Nugen, S.R., Rotello, V.M., 2017. Integrating recognition elements with nanomaterials for bacteria sensing. Chemical Society Reviews 46(5), 1272-1283.

Choi, E.-Y., Han, T.H., Hong, J., Kim, J.E., Lee, S.H., Kim, H.W., Kim, S.O., 2010. Noncovalent functionalization of graphene with end-functional polymers. Journal of Materials Chemistry 20(10), 1907-1912.

Edberg, S.C., Rice, E.W., Karlin, R.J., Allen, M.J., 2000. Escherichia coli: the best biological drinking water indicator for public health protection. Journal of Applied Microbiology 88(S1), 106S-116S.

Geim, A.K., Novoselov, K.S., 2007. The rise of graphene. Nat Mater 6(3), 183-191.

Ghosh, T., Biswas, C., Oh, J., Arabale, G., Hwang, T., Luong, N.D., Jin, M., Lee, Y.H., Nam, J.-D., 2012. Solution-Processed Graphite Membrane from Reassembled Graphene Oxide. Chemistry of Materials 24(3), 594-599.

Hahn, M.A., Tabb, J.S., Krauss, T.D., 2005. Detection of Single Bacterial Pathogens with Semiconductor Quantum Dots. Analytical Chemistry 77(15), 4861-4869.

Hassan, A.-R.H.A.-A., de la Escosura-Muñiz, A., Merkoçi, A., 2015. Highly sensitive and rapid determination of Escherichia coli O157:H7 in minced beef and water using electrocatalytic gold nanoparticle tags. Biosensors and Bioelectronics 67, 511-515.

He, Q., Wu, S., Yin, Z., Zhang, H., 2012. Graphene-based electronic sensors. Chemical Science 3(6), 1764-1772.

Jazayeri, M.H., Amani, H., Pourfatollah, A.A., Pazoki-Toroudi, H., Sedighimoghaddam, B., 2016. Various methods of gold nanoparticles (GNPs) conjugation to antibodies. Sensing and Bio-Sensing Research 9(Supplement C), 17-22.

Jung, I., Dikin, D.A., Piner, R.D., Ruoff, R.S., 2008. Tunable Electrical Conductivity of Individual Graphene Oxide Sheets Reduced at "Low" Temperatures. Nano Letters 8(12), 4283-4287.

Kang, D.-K., Ali, M.M., Zhang, K., Huang, S.S., Peterson, E., Digman, M.A., Gratton, E., Zhao, W., 2014. Rapid detection of single bacteria in unprocessed blood using Integrated Comprehensive Droplet Digital Detection 5, 5427.

Kellici, S., Acord, J., Ball, J., Reehal, H.S., Morgan, D., Saha, B., 2014. A single rapid route for the synthesis of reduced graphene oxide with antibacterial activities. RSC Advances 4(29), 14858-14861.

Kumar, P.V., Bardhan, N.M., Chen, G.-Y., Li, Z., Belcher, A.M., Grossman, J.C., 2016. New insights into the thermal reduction of graphene oxide: Impact of oxygen clustering. Carbon 100(Supplement C), 90-98.

Labib, M., Zamay, A.S., Kolovskaya, O.S., Reshetneva, I.T., Zamay, G.S., Kibbee, R.J., Sattar, S.A., Zamay, T.N., Berezovski, M.V., 2012. Aptamer-Based Viability Impedimetric Sensor for Bacteria. Analytical Chemistry 84(21), 8966-8969.

Laczka, O., Baldrich, E., Muñoz, F.X., del Campo, F.J., 2008. Detection of Escherichia coli and Salmonella typhimurium Using Interdigitated Microelectrode Capacitive Immunosensors: The Importance of Transducer Geometry. Analytical Chemistry 80(19), 7239-7247.

Lee, A., Mirrett, S., Reller, L.B., Weinstein, M.P., 2007. Detection of Bloodstream Infections in Adults: How Many Blood Cultures Are Needed? Journal of Clinical Microbiology 45(11), 3546-3548.

Li, F., Zhao, Q., Wang, C., Lu, X., Li, X.-F., Le, X.C., 2010. Detection of Escherichia coli O157:H7 Using Gold Nanoparticle Labeling and Inductively Coupled Plasma Mass Spectrometry. Analytical Chemistry 82(8), 3399-3403.

Lim, J.Y., Yoon, J.W., Hovde, C.J., 2010. A Brief Overview of Escherichia coli O157:H7 and Its Plasmid O157. Journal of microbiology and biotechnology 20(1), 5-14.

Liu, S., Guo, X., 2012. Carbon nanomaterials field-effect-transistor-based biosensors. NPG Asia Mater 4, e23.

Marcano, D.C., Kosynkin, D.V., Berlin, J.M., Sinitskii, A., Sun, Z., Slesarev, A., Alemany, L.B., Lu, W., Tour, J.M., 2010. Improved Synthesis of Graphene Oxide. ACS Nano 4(8), 4806-4814.

Martínez, M.T., Tseng, Y.-C., Ormategui, N., Loinaz, I., Eritja, R., Bokor, J., 2009. Label-Free DNA Biosensors Based on Functionalized Carbon Nanotube Field Effect Transistors. Nano Letters 9(2), 530-536.

Miranda, O.R., Li, X., Garcia-Gonzalez, L., Zhu, Z.-J., Yan, B., Bunz, U.H.F., Rotello, V.M., 2011. Colorimetric Bacteria Sensing Using a Supramolecular Enzyme–Nanoparticle Biosensor. Journal of the American Chemical Society 133(25), 9650-9653.

Ohno, Y., Maehashi, K., Matsumoto, K., 2010. Label-Free Biosensors Based on Aptamer-Modified Graphene Field-Effect Transistors. Journal of the American Chemical Society 132(51), 18012-18013.

Pandey, A., Gurbuz, Y., Ozguz, V., Niazi, J.H., Qureshi, A., 2017. Graphene-interfaced electrical biosensor for label-free and sensitive detection of foodborne pathogenic E. coli O157:H7. Biosensors and Bioelectronics 91, 225-231.

Schedin, F., Geim, A.K., Morozov, S.V., Hill, E.W., Blake, P., Katsnelson, M.I., Novoselov, K.S., 2007. Detection of individual gas molecules adsorbed on graphene. Nat Mater 6(9), 652-655.

Schmid, M., Shishkin, M., Kresse, G., Napetschnig, E., Varga, P., Kulawik, M., Nilius, N., Rust, H.P., Freund, H.J., 2006. Oxygen-Deficient Line Defects in an Ultrathin Aluminum Oxide Film. Physical Review Letters 97(4), 046101.

Sepunaru, L., Tschulik, K., Batchelor-McAuley, C., Gavish, R., Compton, R.G., 2015. Electrochemical detection of single E. coli bacteria labeled with silver nanoparticles. Biomaterials Science 3(6), 816-820.

Vanaja, Sivapriya K., Russo, Ashley J., Behl, B., Banerjee, I., Yankova, M., Deshmukh, Sachin D., Rathinam, Vijay A.K., 2016. Bacterial Outer Membrane Vesicles Mediate Cytosolic Localization of LPS and Caspase-11 Activation. Cell 165(5), 1106-1119.

Wang, Y., Knoll, W., Dostalek, J., 2012. Bacterial Pathogen Surface Plasmon Resonance Biosensor Advanced by Long Range Surface Plasmons and Magnetic Nanoparticle Assays. Analytical Chemistry 84(19), 8345-8350.

Wu, G., Meyyappan, M., Lai, K.W.C., 2016. Graphene field-effect transistors-based biosensors for Escherichia coli detection. 2016 IEEE 16th International Conference on Nanotechnology (IEEE-NANO), pp. 22-25.

Yoo, S.M., Lee, S.Y., Optical Biosensors for the Detection of Pathogenic Microorganisms. Trends in Biotechnology 34(1), 7-25.

Zang, Y., Huang, D., Di, C.-a., Zhu, D., 2016. Device Engineered Organic Transistors for Flexible Sensing Applications. Advanced Materials, n/a-n/a.

Zhang, Y., Tan, Y.-W., Stormer, H.L., Kim, P., 2005. Experimental observation of the quantum Hall effect and Berry's phase in graphene. Nature 438(7065), 201-204.

Zhao, X., Hilliard, L.R., Mechery, S.J., Wang, Y., Bagwe, R.P., Jin, S., Tan, W., 2004. A rapid bioassay for single bacterial cell quantitation using bioconjugated nanoparticles. Proceedings of the National Academy of Sciences of the United States of America 101(42), 15027-15032.

Zhou, G., Chang, J., Cui, S., Pu, H., Wen, Z., Chen, J., 2014. Real-Time, Selective Detection of Pb2+ in Water Using a Reduced Graphene Oxide/Gold Nanoparticle Field-Effect Transistor Device. ACS Applied Materials & Interfaces 6(21), 19235-19241.

Zhu, C., Yang, G., Li, H., Du, D., Lin, Y., 2015. Electrochemical Sensors and Biosensors Based on Nanomaterials and Nanostructures. Analytical Chemistry 87(1), 230-249.

Highlights

- A graphene-based FET is demonstrated for real-time detection of *E. coli*.
- The device is passivated with ultrathin Al_2O_3 for improved performance.
- The negative charge on *E. coli* surface modulates the FET channel conductivity.
- The biosensor could detect a single *E. coli* within 50 s in 1 µL sample.
- The biosensor was successfully demonstrated for *E. coli* detection in river water.